ISSN 1936-878X/10/$36.00
PUBLISHED BY ELSEVIER INC.
DOI:10.1016/j.jcmg.2009.12.011

iREVIEWS

STATE-OF-THE-ART PAPERS

Heart Failure With Normal Ejection Fraction: The Complementary Roles of Echocardiography and CMR Imaging

Darryl P. Leong, MBBS,*† Carmine G. De Pasquale, MBBS, PhD,*‡
Joseph B. Selvanayagam, MBBS, DPhil*‡
Adelaide, Australia

Heart failure with normal ejection fraction (HFNEF), previously referred to as diastolic heart failure, has increased in prevalence as a cause of heart failure, now accounting for up to 50% of all cases. Contrary to initial evidence, the prognostic outlook in HFNEF may be similar to that of heart failure with reduced ejection fraction. According to current consensus statements, the diagnosis of HFNEF requires the demonstration of relatively preserved systolic left ventricular function and evidence of diastolic dysfunction. Noninvasive imaging techniques now permit evaluation of these parameters without need for cardiac catheterization in the large majority of patients. Echocardiography is the modality of choice in the evaluation of diastolic function but suffers from limitations in its assessment of systolic function. Cardiac magnetic resonance (CMR) imaging is the gold standard in the volumetric quantification of systolic function; however, it has limitations in its ability to characterize diastolic function. This report aims to review the strengths and weaknesses of both imaging modalities in the diagnosis of HFNEF. With regards to echocardiography, it will specifically describe limitations in measuring left ventricular ejection fraction, describe novel techniques to assess systolic function such as tissue velocity and strain analysis, and will review the measurements used in the evaluation of diastolic function. With respect to CMR, this review will highlight its value in the assessment of systolic left ventricular function, will review ancillary CMR findings that may support the diagnosis of HFNEF such as tissue characterization, and will provide a brief overview of CMR techniques to assess diastolic function. We propose that these 2 modalities may play a complementary role in the diagnosis of HFNEF. The importance of imaging in the diagnosis of HFNEF extends to both the individual patient and to clinical trials of therapies for this condition. (J Am Coll Cardiol Img 2010;3:409–20) © 2010 by the American College of Cardiology Foundation

From *Flinders Medical Centre, Adelaide, SA, Australia; †University of Adelaide, Adelaide, SA, Australia; and ‡Flinders University, Adelaide, SA, Australia. Dr. Leong is supported by a Medical Postgraduate Scholarship funded jointly by the National Health and Medical Research Council of Australia and the National Heart Foundation of Australia, and is the recipient of a Dawes Scholarship from the Royal Adelaide Hospital.

Manuscript received August 20, 2009; revised manuscript received December 1, 2009, accepted December 15, 2009.

JACC: CARDIOVASCULAR IMAGING, VOL. 3, NO. 4, 2010
APRIL 2010:409–20

Heart failure with normal ejection fraction (HFNEF) refers to the clinical syndrome of heart failure in the presence of normal left ventricular (LV) ejection fraction. Three conditions must be fulfilled for its diagnosis: 1) the presence of symptoms or signs of heart failure; 2) the presence of normal or mildly abnormal systolic function; and 3) evidence of diastolic LV dysfunction (1). With the aging population, and increasing prevalence of hypertension, diabetes, and obesity, HFNEF now accounts for up to 50% of all cases (2). Despite initial studies suggesting a better prognosis than heart failure with reduced ejection fraction (HFREF), more recent evidence suggests similar prognostic outlook with both entities (3). A recent consensus statement proposed replacement of the terms *systolic* and *diastolic heart failure* with HFREF and HFNEF, respectively, as the former implies mutually exclusive mechanisms, whereas diastolic dysfunction is highly prevalent in systolic heart failure (4), and there is evidence to suggest reduced systolic tissue velocities in diastolic heart failure (5). Moreover, published guidelines on the diagnosis of HFNEF (1) uniformly require objective evidence of diastolic LV dysfunction in addition to clinical features of heart failure and LV ejection fraction (LVEF) >50%. Thus, imaging modalities play a pivotal role in 2 of the 3 diagnostic criteria of HFNEF. Recent advances in echocardiographic and cardiac magnetic resonance (CMR) imaging techniques allow more accurate characterization of cardiac structure and function, and permit more certain diagnosis of HFNEF.

ABBREVIATIONS AND ACRONYMS

2D = 2-dimensional

3D = 3-dimensional

AF = atrial fibrillation

CMR = cardiac magnetic resonance

HFNEF = heart failure with normal ejection fraction

HFREF = heart failure with reduced ejection fraction

LA = left atrial

LGE = late gadolinium enhancement

LV = left ventricular

LVEF = left ventricular ejection fraction

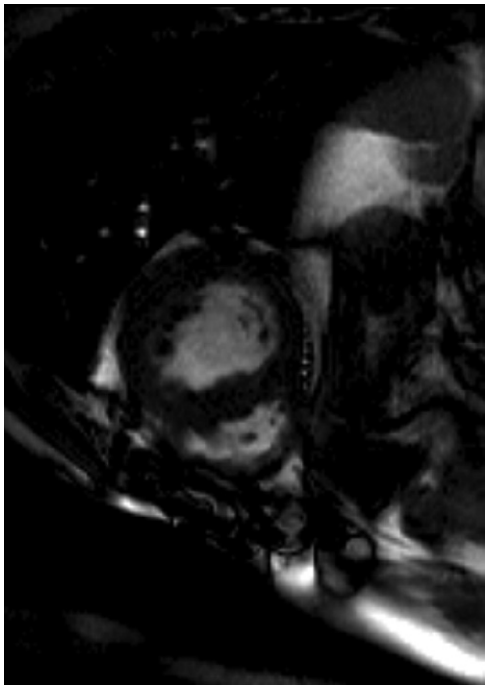

Figure 1. Short-Axis White Blood CMR Image Demonstrating Concentric LVH

This end-diastolic short-axis cine cardiac magnetic resonance (CMR) image demonstrates concentric thickening of the left ventricular walls. The high spatial resolution and signal-to-noise ratio of cardiac magnetic resonance allows tightly reproducible measurement of left ventricular wall thickness and total left ventricular myocardial mass. See Online Videos 1 and 2. LVH = left ventricular hypertrophy.

Pathophysiology of Diastolic Dysfunction

At a macroscopic level, HFNEF is distinguished from HFREF by concentric LV remodeling rather than eccentric. Concentric remodeling refers to maintenance or increase in LV wall thickness relative to chamber size (Fig. 1), whereas in eccentric remodeling, there is LV cavity dilation, and relative wall thickness is diminished.

Diastolic dysfunction is characterized pathophysiologically by increased LV stiffness (6). Consequently, with exercise, there is an inability to augment LV end-diastolic volume despite increasing LV end-diastolic pressure. The outcome of increased LV stiffness is reflected in the hemodynamic changes that are most widely used to assess diastolic function. In normal diastole, LV untwisting—a vigorous and active process—sucks blood from the left atrium into the left ventricle. Seventy percent to 80% of LV filling under these circumstances occurs in early diastole, with atrial contraction accounting for the remaining 20% to 30%. With the development of early diastolic dysfunction, the proportion of LV filling permitted to occur in early diastole is reduced. The relative importance of atrial contraction is thus increased—so-called grade I diastolic dysfunction. As diastolic dysfunction worsens, pressure mounts within the left atrium, such that immediately following mitral valve opening, blood is forced under positive pressure, rather than sucked by negative pressure, into the left ventricle. Although the proportion of LV filling occurring in early diastole returns to normal, the underlying physiology is not normal, hence the designation of pseudonormal LV filling, or grade II diastolic dysfunction. Grade III diastolic dysfunction is charac-

terized by very abrupt flow of blood from left atrium into left ventricle, but with reversibility with the Valsalva maneuver. Grade IV diastolic dysfunction is characterized by irreversibility with the Valsalva maneuver.

Assessment of Systolic LV Function

Echocardiography. A sine qua non in the diagnosis of HFNEF is the establishment of normal LVEF. Traditional measurement of LVEF by 2-dimensional (2D) echocardiography relies on clear endocardial definition, which is lacking in up to 31% cases (7), particularly when intravenous contrast is not utilized. LVEF in patients with clinical heart failure is a unimodally distributed continuous variable. Thus, the cutoff of 50% to dichotomize HFNEF from HFREF is somewhat arbitrary. Nonetheless, reproducible assessment of LV volumes is crucial in delineating the predominant pathogenic mechanisms underlying a patient's heart failure. Even in the hands of expert echocardiographic laboratories, there is considerable variability in the estimation of LVEF (8). Furthermore, there is poor agreement between Simpson's biplane technique and CMR imaging, the imaging gold standard for estimation of cardiac volumes, with Bland-Altman limits of agreement of up to ±20% among a sample of heart failure patients (7).

In 3-dimensional (3D) echocardiography, data are acquired over 4 to 6 cardiac cycles then synthesized into a single so-called full-volume dataset. This can then be manipulated or cropped to obtain nonforeshortened planes through the left ventricle, thus permitting more accurate estimation of chamber volumes. Three-dimensional echocardiography boasts superior reproducibility and closer approximation to CMR than 2D echo in the measurement of LVEF (9). Despite minimal bias compared with CMR, 3D echo has slightly greater variability (10). This may relate to poorer spatial resolution and endocardial definition, which is suboptimal in up to 20% of cases, and is associated with less reliable measurement of LV volumes compared with non–endocardial-dependent techniques (11). Three-dimensional echocardiography and CMR both require the patient to breath-hold during image acquisition, which can prove difficult in those dyspneic at rest.

Although accurate and reproducible measurement of LVEF is clearly desirable, it is not always feasible in clinical practice, where patient characteristics often differ greatly from those studied in the research setting. Obstacles such as the inability to adequately position bed-bound patients, ventilator dependency in the intensive care unit, and comorbidities such as chronic obstructive pulmonary disease and obesity frequently render accurate measurement of LVEF limited using conventional echo techniques. Contrast echocardiography and tissue Doppler imaging may potentially have a role to play in this setting. Contrast-enhanced 2D echocardiography has similar accuracy to noncontrast 3D echocardiography (12). Contrast-enhanced 3D echocardiography may yield even superior results (12). Peak systolic tissue velocity (Sm) by pulse wave tissue Doppler at the mitral annulus has been shown to correlate with LVEF. Sm <7 cm/s predicts LVEF $<45\%$ with sensitivity 93% and specificity 87% (13). Tissue velocity in this location represents an integral of longitudinal cardiac motion from base to apex. The advantage of tissue Doppler imaging is that it is not reliant on good 2D image quality and has good reproducibility.

Speckle tracking technology provides another echocardiographic means to evaluate systolic LV function. It relies on tracking small myocardial regions of interest, each with a relatively unique appearance owing to its pattern of acoustic backscatter, through space from frame to frame. This then permits calculation of strain—tissue deformation—on a regional basis. Current software allows regional strain scores to be averaged to yield a global strain score. This score has been proven an accurate index of systolic LV function in chronic ischemic heart disease (14). Global strain score's advantage over LVEF as an index is its reproducibility, although its prognostic role remains to be determined. Furthermore, strain analysis permits interrogation of myocardial deformation in any cardiac axis. Wang et al. (15) recently demonstrated that longitudinal and radial systolic strains are reduced in diastolic heart failure although LV twist is preserved.

CMR imaging. CMR has rapidly become the imaging method of choice and the gold standard in the assessment of systolic cardiac function of both normal and abnormal left ventricles (7). With regard to measurement of global LV systolic function, given its 3D nature and an order of magnitude greater signal-to-noise ratio, CMR is highly superior to 2D echo (7). Given its greater reproducibility in measuring LVEF over 2D echo, the potential for erroneously categorizing heart failure is markedly lessened. This imaging is typically performed in, although not limited to, the conventional short-axis

JACC: CARDIOVASCULAR IMAGING, VOL. 3, NO. 4, 2010
APRIL 2010:409–20

views (Online Video 1) and the 3 cardinal long-axis views (Online Video 2). The ability of CMR to image in any plane without the need for optimal imaging windows allows for unprecedented flexibility for the interrogation of abnormal heart structures.

Cine images are obtained using steady-state free precession sequences, which provide images of higher signal to noise (than older sequences such as gradient echo), and hence exceptional delineation of the blood–myocardium interface. This allows for accurate and reproducible quantitative assessment of chamber dimensions and systolic function using manual or semiautomated planimetry techniques.

Visual inspection of LV and right ventricular architecture identifies patterns of regional or diffuse wall thinning and concentric or asymmetric hypertrophy. Pericardial thickness and calcification can be assessed. The spatial resolution with which this can be achieved by CMR is useful in distinguishing pericardial constriction from restrictive cardiomyopathy, both of which may result in features of heart failure with normal ejection fraction. Tomographic imaging is an important adjunct to echocardiographic characterization of hemodynamics, which forms the cornerstone of diagnosing pericardial constriction, especially given the observation that constriction may occur in the absence of pericardial thickening.

CMR tagging is a technique by which a radiofrequency pulse is applied to LV myocardium in the form of grid lines. The tagged grid deforms as the saturated myocardium moves throughout the cardiac cycle, allowing regional strain to be visualized and quantified. The tag is generally applied at the onset of systole, triggered by the ECG R-wave, and fades during the cardiac cycle as the magnetization recovers towards equilibrium as a result of spin-lattice, or T1, relaxation. Measurement of strain is suited to quantifying regional systolic LV function.

The tissue phase mapping technique allows the determination of 3D velocity tensors over the cardiac cycle, i.e., for rotation, radial, and longitudinal movement, with a pixel-by-pixel spatial resolution nearing that of "conventional" cine CMR (16). This has been investigated in clinical studies in both patients and volunteers, and newer navigator sequences (obviating the need for breath-holding, and hence with the potential for improving spatial resolution) have been developed. Displacement-encoded imaging using stimulated echoes (DENSE) can also provide information on myocardial displacement, velocity, and strain (17).

Table 1. Characteristic Patterns of LGE and Ancillary Findings on CMR Imaging in Various Disease States That May Present as HFNEF

Disease (Ref. #)	Pattern of Late Gadolinium Enhancement	Prevalence of Late Gadolinium Enhancement*	Ancillary Findings
HCM (18,20)	Mid-wall within hypertrophied segments in patchy distribution Most consistently at anterior and posterior junction of interventricular septum and right ventricular free wall	79%–81%	LV hypertrophy, usually asymmetric
Fabry disease (21)	Most often basal inferolateral wall Subendocardium usually spared	50%	LV hypertrophy—may be indistinguishable from HCM. Biopsy or genetic testing confirms diagnosis
Amyloidosis (22)	Diffuse Subendocardial but traversing arterial territories	69%	Multiple images of the same view using different inversion times may allow demonstration of diffuse early nulling of myocardial signal to suggest amyloidosis
Pericardial constriction	The presence of pericardial enhancement suggests ongoing inflammation	—	Pericardial thickness >4 mm is consistent with the diagnosis, and >5 mm has high specificity

*Quoted figures are from the cited references and represent the best available estimate of late gadolinium enhancement, although actual prevalence may vary with the population studied.
CMR = cardiac magnetic resonance; HCM = hypertrophic cardiomyopathy; HFNEF = heart failure with normal ejection fraction; LGE = late gadolinium enhancement; LV = left ventricular.

Tissue Characterization

The development of the late gadolinium enhancement (LGE) CMR technique (LGE-CMR) has revolutionized the role of CMR in clinical and research practice. It has a potential role in the context of HFNEF, in identifying specific patterns of fibrosis and scarring in many of the cardiomyopathy states that may initially present with HFNEF (18,19). This is summarized in Table 1. There is a high prevalence (79% to 81%) of late gadolinium enhancement in hypertrophic cardiomyopathy (18,20). Its distribution is typically mid-wall within hypertrophied segments, and is particularly prominent at the junction of the interventricular septum and right ventricular free wall (20) (Fig. 2). Fabry disease, caused by X-linked alpha-galactosidase deficiency, may be difficult to distinguish echocardiographically from hypertrophic cardiomyopathy. This distinction is important because disease-targeted therapy may improve outcome in Fabry

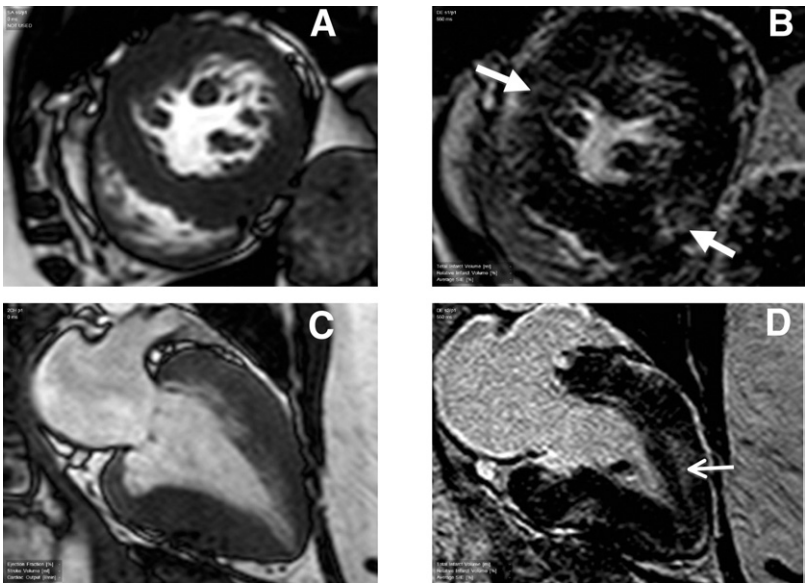

Figure 2. End-Diastolic Images From a Patient With Hypertrophic Cardiomyopathy

(A) Short-axis white blood cardiac magnetic resonance (CMR) image demonstrating asymmetric septal hypertrophy. **(B)** Short-axis late gadolinium-enhancement CMR image demonstrating increased signal intensity at the junction of the interventricular septum and right ventricular free wall **(arrows)**. **(C)** Vertical long-axis white blood CMR image demonstrating left ventricular hypertrophy. **(D)** Vertical long-axis late gadolinium-enhancement CMR image demonstrating increased signal intensity in the anterior wall **(arrow)**. See Online Video 3.

disease. LGE occurs in 50% of cases, and if present, usually affects the basal inferolateral wall, sparing the subendocardium (21). Amyloidosis has been found to be associated with qualitative global and subendocardial gadolinium enhancement of the myocardium. A recent landmark study found that subendocardial longitudinal relaxation time (T1) in amyloid patients was shorter than in controls, and was correlated with markers of increased myocardial amyloid load, such as LV mass, wall thickness, interatrial septal thickness, and diastolic function. Global subendocardial LGE was found in approximately two-thirds of patients (22). The T2* CMR technique, which is noncontrast-dependent, has been shown to be valuable in the quantification of myocardial iron deposition in hemochromatosis (23).

Assessment of Left Atrial Volume

Left atrial (LA) size is an important prognostic marker in a number of cardiovascular disease states (24,25). It can be considered as an end point of cumulative LV insult. LA dilation can help discriminate normal from pseudonormal LV filling (26), and its finding in the appropriate clinical setting supports the diagnosis of HFNEF (27). A large cross-sectional study has shown the association between LA volume (indexed to body surface area) and grade of diastolic dysfunction with an area under the receiver-operator characteristic curve of 0.81 to detect grade II diastolic dysfunction (28).

Echocardiography. As with assessment of LV cavity size, quantification of LA size has progressed from single-dimension measurement by M-mode echocardiography to single-plane and biplane estimation of area and volume. Prognostic discriminatory power increases with each step's increase in data. Among 2D techniques used to assess LA volume Simpson's biplane and the area-length method have the closest correlation, whereas the prolate-ellipsoid technique underestimates LA volume (29). More recently, 3D echocardiography has been used to evaluate LA volume (30). This technique has superior test-retest reliability and inter- and intraobserver variability to other echocardiographic techniques (31).

Magnetic resonance imaging. Early studies determined reference ranges for LA dimensions and area (32). Subsequent studies examined the accuracy of measurement of LA volume by either a modified bi-plane Simpson's technique from the horizontal and vertical long axes (33), or by measurement from a short axis stack (34). The inter- and intraobserver variability and interstudy variability tend to be greater when LA volume is measured using the modified Simpson's technique (35). The appendage

Table 2. Echocardiographic Classification of Grades of Diastolic Dysfunction

Parameter	Normal	Mild Dysfunction (Grade 1)	Moderate Dysfunction (Grade 2)	Severe Dysfunction (Grade 3)	Severe Dysfunction (Grade 4)
Transmitral PW Doppler					
E/A	1–1.5	<1	1–1.5	>2	>2.5
DT (ms)	140–250	>250	140–250	<140	<140
TDI					
E′ (cm/s)	≥7	<7	<7	<5	<5
Valsalva	Negative	Positive	Positive	Positive	Negative
LAVI (ml/m^2)	22 ± 6	>28	>28	>35	>40
Pulmonary venous flow	S ≥ D	S >> D	S < D	S << D	S << D
Mitral in-flow propagation velocity (cm/s)	≥50	<50	<50	<50	<50

D = peak D-wave velocity; DT = deceleration time; E/A = ratio of E- to A-wave velocities; LAVI = left atrial volume indexed to body surface area; PW = pulse wave; S = peak S-wave velocity; TDI = pulse wave tissue Doppler imaging at the septal mitral annulus.

is generally included in the LA volume, but pulmonary veins are excluded.

Assessment of LV Mass

There is a well-recognized association between LV mass and adverse cardiovascular outcomes and even sudden cardiac death (36). This relationship persists after adjustment for conventional cardiovascular risk factors. This association likely holds true because LV mass, like LA volume, represents an end point of cumulative LV insult. Although not a diagnostic criterion for HFNEF, increased LV mass provides supportive evidence. Furthermore, it is conceptually attractive to quantify LV mass as it relates directly to the pathological process underlying HFNEF, although further investigation is needed to truly relate the anatopathologic defect of LV mass to that of the physiologic perturbation of diastolic function.

Echocardiography. Early echocardiographic techniques for measuring LV mass that relied on M-mode have been superseded by 2D and, more recently, 3D techniques. Each advance in echocardiographic methodology has resulted in fewer inherent assumptions and thus more accurate and reproducible measurement of LV mass. 3D echocardiographic measurement of LV mass is more reproducible than 2D, and approximates CMR more closely (37), whereas 2D techniques suffer from wide limits of agreement (38).

CMR. CMR is the noninvasive gold standard for measurement of LV mass (39) and has been validated against cadaveric measurements (40). Normal ranges for LV mass by CMR have been published (41). The technique for measurement of LV myocardial volume requires manual or semiautomated endo- and epicardial border tracing. LV mass is calculated by multiplying this volume by 1.05g/cm^3 (the specific density of myocardium). The greater accuracy and reproducibility of CMR in the measurement of LV mass allow smaller changes to be detected (Online Videos 1 to 3). This provides greater sensitivity to measure the effects of disease progression or efficacy of disease therapy.

Assessment of Diastolic LV Function

Echocardiography. Echocardiography is the imaging technique of choice in evaluation of diastolic function. Among the parameters available for echocardiographic assessment of diastolic function (Table 2), transmitral flow velocities and tissue Doppler imaging are the quickest to acquire and have the lowest interobserver variability (42). In healthy, young individuals, most LV filling occurs in early diastole, resulting in a prevailing E-wave. With aging or diastolic dysfunction, increasing LV stiffness and impaired diastolic LV untwisting reduces early LV filling, thus resulting in a predominant A-wave. As diastolic dysfunction progresses to pseudonormality, LA pressure rises, and early LV filling increases in proportion. Despite an E/A ratio >1, the pathophysiological distinction from normality is that early LV filling is from blood being forced in rather than being sucked in. In grade III diastolic dysfunction, the E/A ratio is >2 and deceleration time <140 ms (Fig. 3). Although the finding of a restrictive transmitral filling profile allows easy recognition of diastolic dysfunction, this pattern is only observed in 10% of cases of HFNEF (4). Occasionally, a triphasic pattern of transmitral filling is observed (Fig. 4) as an L-wave: antegrade flow resulting in a Doppler signal between the E and A waves, during what is normally diastasis.

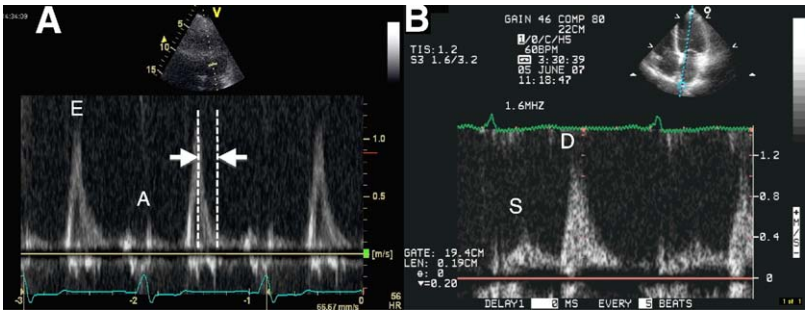

Figure 3. Doppler Evaluation of a Patient With Restrictive LV Filling

(A) Transmitral pulsed wave Doppler at mitral valve leaflet tips demonstrating E/A ratio >2 and brief deceleration time **(arrows)**. **(B)** Pulsed wave Doppler at the ostium of the right upper pulmonary vein showing S-wave << D-wave. E/A = ratio of E- to A-wave velocities; LV = left ventricular.

Although not necessarily pathognomonic for severe diastolic dysfunction, the L-wave has a predilection for occurrence in those with significant LV pathology, and thus may be supportive of diastolic dysfunction (43).

A challenge in diastology is the distinction of pseudonormal filling from normal. Of assistance in this regard are (Table 2): 1) the Valsalva maneuver, which results in reversal in E/A ratio in pseudonormality, but not in normality (Fig. 5B); 2) tissue Doppler imaging at the mitral annulus, where E′ <7 cm/s suggests diastolic dysfunction, and E′ <5 cm/s strongly supports it (Fig. 5C); 3) pulmonary venous Doppler (Fig. 5D); 4) propagation of mitral in-flow towards the apex using color M-mode (44); 5) systolic LV function—if impaired, suggests concomitant diastolic dysfunction; 6) LV hypertrophy, which suggests diastolic dysfunction; and 7) LA dilation, which also supports the diagnosis of diastolic dysfunction. Caution must be exercised relying solely on E/A ratio: following cardioversion or spontaneous reversion to sinus rhythm from atrial fibrillation the A-wave is reduced owing to atrial stunning. This can give a misleadingly high E/A ratio. Moderate or greater mitral valve disease poses a similar caveat.

Peak early diastolic mitral velocity (E) is influenced by LA pressure, age, and LV relaxation, whereas peak diastolic mitral annular tissue velocity (E′) is governed by age and LV relaxation. Thus the E/E′ ratio is, theoretically, a measure of LA pressure. E/E′ has been shown to have a better correlation with LV end-diastolic pressure (LVEDP) than other echocardiographic indices, with a ratio >15 predicting elevated mean LVEDP (45). It is again important to be aware of a technique's limitations. If septal motion is abnormal, for instance as a result of right ventricular pacing or left bundle branch block, E/E′ has been shown unreliable for the prediction of pulmonary capillary wedge pressure (46). Nonetheless, in a study of patients 1.6 days following myocardial infarction, 42% of which were anterior, E/E′ was a superior prognostic index to other clinical and echocardiographic parameters (47).

CMR. In contrast to the wealth of studies in LV systolic dysfunction, there is relative inexperience in CMR assessment of diastolic LV function. Nonetheless, a number of CMR techniques have been used to evaluate diastolic function. Peak LV filling rates in early and late diastole can be measured by rates of change in chamber volume—a technique made possible by CMR's high spatial resolution. It has been demonstrated that their ratio decreases

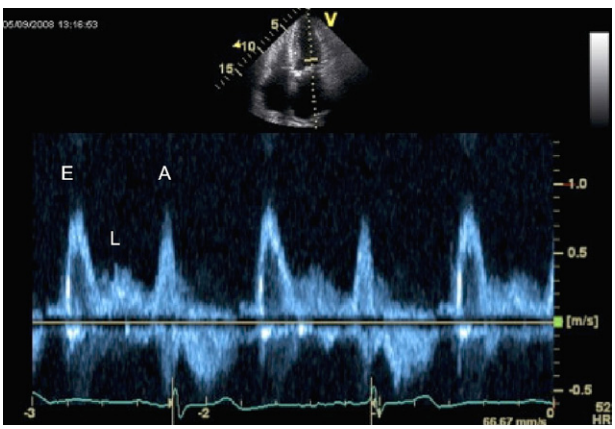

Figure 4. Diastolic L-Wave on Transmitral Doppler Echocardiography

Transmitral pulsed wave Doppler at mitral valve leaflet tips in a patient with pseudonormal left ventricular filling. An L-wave is seen as antegrade flow occurring between the E and A waves.

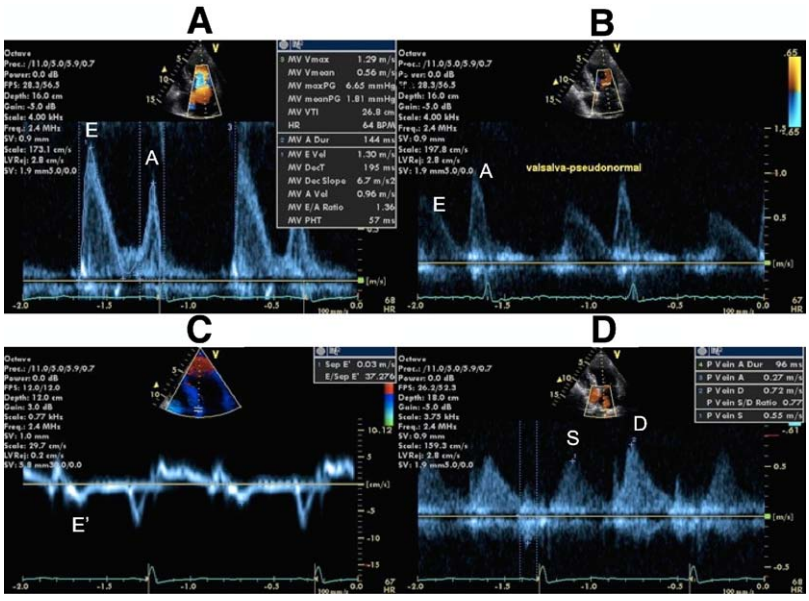

Figure 5. Doppler Evaluation of a Patient With Pseudonormal LV Filling

(A) Transmitral pulsed wave Doppler at mitral valve leaflet tips. **(B)** Transmitral pulsed wave Doppler at mitral valve leaflet tips during Valsalva maneuver illustrating E/A reversal. **(C)** Pulsed-wave tissue Doppler imaging at the septal mitral annulus demonstrating reduced diastolic E′ velocity. **(D)** Pulsed wave Doppler at the ostium of the right upper pulmonary vein showing S-wave < D-wave. LV = left ventricular.

with age in healthy individuals, in a manner analogous to E/A ratio by transmitral Doppler echo (48). Volume-derived indices such as peak early and late LV filling rate and time to peak early LV filling have been promoted as sensitive markers of diastolic dysfunction (49), but their measurement remains highly time-consuming with present software and impractical from a clinical perspective.

Blood flow velocity can be measured by CMR. Phase-contrast imaging, in which the spin phase shift is used to estimate transmitral blood flow velocity, has demonstrated at least moderate correlation with echocardiography (50,51), although 95% confidence limits on Bland-Altman analysis are wide. Velocities measured by CMR tend to be lower than by echocardiography as a consequence of the lower temporal resolution of CMR. Temporal resolution may be improved by reducing number of views/segment; however, this requires longer breath-hold times.

Studies have employed myocardial grid tagging to demonstrate abnormalities in LV untwisting in diastole in conditions such as aortic stenosis (52). To date, the major limitation in myocardial grid tagging for the assessment of diastolic function has been the fading of grid lines over the course of the cardiac cycle. In a large population study of subjects without known cardiovascular disease, early diastolic strain rate (the first temporal derivative of strain) could be measured in 80% of segments analyzed (53). Atrial-induced strain rate could be assessed in only 32% of patients. In the remainder, tag lines faded in intensity, precluding analysis. Although this study found early diastolic strain rate inversely proportional to indexed LV mass, it highlights the current limitations of CMR in assessing diastolic function. Imaging sequences with higher temporal resolution have been shown to increase the proportion of the cardiac cycle that can be analyzed over older fast-gradient echo sequences. A 3.0-T CMR has been shown to produce better tag persistence through the cardiac cycle than 1.5-T and might have a role in the future (54).

Velocity-encoded CMR or tissue-phase mapping has been used to evaluate regional systolic and diastolic tissue velocities in an analogous manner to echocardiography (55,56). It has superior spatial resolution to grid tagging because the number of grid lines that can be placed on the myocardium limits the latter. Tissue-phase mapping also encompasses more of the cardiac cycle than grid tagging. Despite its feasibility, tissue-phase mapping has not gained widespread popularity in the evaluation of diastolic function, mainly due to poorer temporal resolution and difficulty with the long breath-hold times required, which is of particular relevance in

the heart failure population. Bergvall et al. (57) have validated tissue-phase mapping during free breathing against grid tagging. Fading of the grid lines in diastole limited the validation of diastolic tissue velocities, however.

In summary, although early studies show promise in CMR assessment of diastolic function, present limitations and the time-consuming nature of data acquisition restrict the widespread implementation of these techniques.

Atrial Fibrillation

Atrial fibrillation (AF) poses a challenge to the evaluation of cardiac function. Variability in cycle length hinders estimation of LV function by any modality because of beat-to-beat variation in LV filling and ejection. Furthermore, loss of the A-wave precludes measurement of the E/A ratio. It is recommended that measurements taken in AF be averaged over at least 5 cardiac cycles, although this may have workflow implications in busy laboratories.

Modest correlation exists between transmitral deceleration and pulmonary capillary wedge pressure, although the clinical utility of this is limited (58). The E/E′ ratio remains of value in the diagnosis of HFNEF in the presence of AF. In a cross-sectional study of patients with HFNEF, septal E/E′ >13 corroborated the diagnosis with sensitivity 81.8% and specificity 89.5% (59). An observational study of nonvalvular AF demonstrated that E/E′ >15 is an independent predictor of mortality (60). Pulmonary venous flow profiles may be of use in AF. A deceleration time of the D-wave >220 ms has been shown to predict mean pulmonary capillary wedge pressure ≤12 mm Hg with 100% sensitivity and specificity (58). Although LA volume reflects prevailing LV function, its discriminatory role in AF is confounded by the fact that AF itself promotes LA dilation.

Future Directions

Present-generation matrix array probes that permit real-time 3D echocardiographic imaging are large in size, rendering them unwieldy. As their dimensions decrease, a greater proportion of individuals will be able to benefit from 3D echocardiography. Current echocardiographic acquisition of myocardial tissue velocity or strain data utilizes sequential images in different 2D planes. The inherent limitation that results is from possible beat-to-beat variability in myocardial function. The development of 3D probes that permit real-time recording of tissue velocity or deformation information may make accurate characterization of all aspects of myocardial function more rapid and reliable.

Nonangulated 3D CMR images of the heart acquired even during free breathing has shown promise in overcoming some of the limitations of CMR estimation of LVEF (61). Emerging CMR techniques that allow mapping of blood flow may allow more accurate characterization of LV filling kinetics (62). The temporal and prognostic relationship between myocardial fibrosis and HFNEF warrants further investigation. Tools such as LGE-CMR and integrated echocardiographic backscatter are available to quantitate myocardial fibrosis, but whether this adds incrementally useful data in the diagnosis of HFNEF is uncertain. The major limitation of LGE in the detection of myocardial fibrosis is that it relies on difference in signal intensity between scarred regions and adjacent normal myocardium. It may thus have reduced sensitivity for diffuse fibrosis. The calculation of a post-contrast myocardial T1 time following imaging a given plane with sequentially increasing inversion times has recently been shown to discriminate heart failure patients from healthy controls even after excluding myocardial segments displaying LGE. This technique shows promise in more sensitive and quantitative evaluation of myocardial fibrosis (63).

Imaging of blood flow propagation and vorticity is currently under development. Its advent will allow greater characterization of the relationship between LV filling and ejection. Lastly, fusion imaging, which integrates data from more than 1 modality, may permit the advantages of different techniques to become fully integrated.

Conclusions

Two of the 3 criteria for diagnosis of HFNEF are dependent on cardiac imaging. Echocardiography and CMR are the 2 modalities that offer the most in this regard because they obtain data on cardiac structure and function, in contrast to scintigraphy. They each have strengths and limitations that at present make them complementary. Echocardiography's high temporal resolution makes it the modality of choice for assessing diastolic function, whereas CMR's high spatial resolution permits precise evaluation of systolic function. Although CMR suffers from limited availability, and contraindications such as implantable metallic devices, its

JACC: CARDIOVASCULAR IMAGING, VOL. 3, NO. 4, 2010
APRIL 2010:409–20

ability to obtain accurate information in patients with poor echocardiographic windows makes it an important alternative in the diagnosis and characterization of heart failure. Each modality has made recent progress to address their respective areas of weakness. If appropriate echo windows are available, 3D echo approaches CMR in the estimation of LVEF. Advances in CMR sequences increasingly allow characterization of diastole. Although both imaging modalities are not necessary for the diagnosis of HFNEF in the majority of cases, uncertainty following 1 scan may be resolved by utilizing the strengths of the other.

Reprint requests and correspondence: Dr. Joseph B. Selvanayagam, Department of Cardiology, Flinders Medical Centre, Bedford Park, SA, Australia 5042. *E-mail: Joseph.Selvanayagam@flinders.edu.au.*

REFERENCES

1. Paulus WJ, Tschope C, Sanderson JE, et al. How to diagnose diastolic heart failure: a consensus statement on the diagnosis of heart failure with normal left ventricular ejection fraction by the Heart Failure and Echocardiography Associations of the European Society of Cardiology. Eur Heart J 2007;28:2539–50.
2. Owan TE, Hodge DO, Herges RM, Jacobsen SJ, Roger VL, Redfield MM. Trends in prevalence and outcome of heart failure with preserved ejection fraction. N Engl J Med 2006; 355:251–9.
3. Bhatia RS, Tu JV, Lee DS, et al. Outcome of heart failure with preserved ejection fraction in a population-based study. N Engl J Med 2006;355:260–9.
4. Bursi F, Weston SA, Redfield MM, et al. Systolic and diastolic heart failure in the community. JAMA 2006; 296:2209–16.
5. Yu CM, Lin H, Yang H, Kong SL, Zhang Q, Lee SW. Progression of systolic abnormalities in patients with "isolated" diastolic heart failure and diastolic dysfunction. Circulation 2002;105: 1195–201.
6. Westermann D, Kasner M, Steendijk P, et al. Role of left ventricular stiffness in heart failure with normal ejection fraction. Circulation 2008;117: 2051–60.
7. Bellenger NG, Burgess MI, Ray SG, et al. Comparison of left ventricular ejection fraction and volumes in heart failure by echocardiography, radionuclide ventriculography and cardiovascular magnetic resonance; are they interchangeable? Eur Heart J 2000;21: 1387–96.
8. Hare JL, Brown JK, Marwick TH. Performance of conventional echocardiographic parameters and myocardial measurements in the sequential evaluation of left ventricular function. Am J Cardiol 2008;101:706–11.
9. Soliman OI, Kirschbaum SW, van Dalen BM, et al. Accuracy and reproducibility of quantitation of left ventricular function by real-time three-dimensional echocardiography versus cardiac magnetic resonance. Am J Cardiol 2008;102:778–83.
10. Sugeng L, Mor-Avi V, Weinert L, et al. Quantitative assessment of left ventricular size and function: side-by-side comparison of real-time three-dimensional echocardiography and computed tomography with magnetic resonance reference. Circulation 2006; 114:654–61.
11. Tighe DA, Rosetti M, Vinch CS, et al. Influence of image quality on the accuracy of real time three-dimensional echocardiography to measure left ventricular volumes in unselected patients: a comparison with gated-SPECT imaging. Echocardiography 2007;24:1073–80.
12. Jenkins C, Moir S, Chan J, Rakhit D, Haluska B, Marwick TH. Left ventricular volume measurement with echocardiography: a comparison of left ventricular opacification, three-dimensional echocardiography, or both with magnetic resonance imaging. Eur Heart J 2009;30:98–106.
13. Ruan Q, Nagueh SF. Usefulness of isovolumic and systolic ejection signals by tissue Doppler for the assessment of left ventricular systolic function in ischemic or idiopathic dilated cardiomyopathy. Am J Cardiol 2006;97:872–5.
14. Gjesdal O, Hopp E, Vartdal T, et al. Global longitudinal strain measured by two-dimensional speckle tracking echocardiography is closely related to myocardial infarct size in chronic ischaemic heart disease. Clin Sci (Lond) 2007;113:287–96.
15. Wang J, Khoury DS, Yue Y, Torre-Amione G, Nagueh SF. Preserved left ventricular twist and circumferential deformation, but depressed longitudinal and radial deformation in patients with diastolic heart failure. Eur Heart J 2008;29:1283–9.
16. Hennig J, Schneider B, Peschl S, Markl M, Krause T, Laubenberger J. Analysis of myocardial motion based on velocity measurements with a black blood prepared segmented gradient-echo sequence: methodology and applications to normal volunteers and patients. J Magn Reson Imaging 1998;8:868–77.
17. Gilson WD, Yang Z, French BA, Epstein FH. Measurement of myocardial mechanics in mice before and after infarction using multislice displacement-encoded MRI with 3D motion encoding. Am J Physiol Heart Circ Physiol 2005;288:H1491-7.
18. Moon JC, McKenna WJ, McCrohon JA, Elliott PM, Smith GC, Pennell DJ. Toward clinical risk assessment in hypertrophic cardiomyopathy with gadolinium cardiovascular magnetic resonance. J Am Coll Cardiol 2003;41:1561–7.
19. McCrohon JA, Moon JC, Prasad SK, et al. Differentiation of heart failure related to dilated cardiomyopathy and coronary artery disease using gadolinium-enhanced cardiovascular magnetic resonance. Circulation 2003;108:54–9.
20. Choudhury L, Mahrholdt H, Wagner A, et al. Myocardial scarring in asymptomatic or mildly symptomatic patients with hypertrophic cardiomyopathy. J Am Coll Cardiol 2002;40:2156–64.
21. Moon JC, Sachdev B, Elkington AG, et al. Gadolinium enhanced cardiovascular magnetic resonance in Anderson-Fabry disease. Evidence for a disease specific abnormality of the myocardial interstitium. Eur Heart J 2003;24:2151–5.
22. Maceira AM, Joshi J, Prasad SK, et al. Cardiovascular magnetic resonance in cardiac amyloidosis. Circulation 2005; 111:186–93.
23. Anderson LJ, Holden S, Davis B, et al. Cardiovascular T2-star (T2*) magnetic resonance for the early diagnosis of myocardial iron overload. Eur Heart J 2001;22:2171–9.
24. Tsang TS, Abhayaratna WP, Barnes ME, et al. Prediction of cardiovascular outcomes with left atrial size: is volume superior to area or diameter? J Am Coll Cardiol 2006;47:1018–23.
25. Ristow B, Ali S, Whooley MA, Schiller NB. Usefulness of left atrial volume index to predict heart failure hospitalization and mortality in ambulatory patients with coronary heart disease and comparison to left ventricular ejection fraction (from the Heart and Soul Study). Am J Cardiol 2008; 102:70–6.

26. De Castro S, Caselli S, Di Angelantonio E, et al. Relation of left atrial maximal volume measured by real-time 3D echocardiography to demographic, clinical, and Doppler variables. Am J Cardiol 2008;101: 1347–52.
27. Yoshida C, Nakao S, Goda A, et al. Value of assessment of left atrial volume and diameter in patients with heart failure but with normal left ventricular ejection fraction and mitral flow velocity pattern. Eur J Echocardiogr 2009;10:278-81.
28. Pritchett AM, Mahoney DW, Jacobsen SJ, Rodeheffer RJ, Karon BL, Redfield MM. Diastolic dysfunction and left atrial volume: a population-based study. J Am Coll Cardiol 2005;45:87–92.
29. Ujino K, Barnes ME, Cha SS, et al. Two-dimensional echocardiographic methods for assessment of left atrial volume. Am J Cardiol 2006;98:1185–8.
30. Maddukuri PV, Vieira ML, DeCastro S, et al. What is the best approach for the assessment of left atrial size? Comparison of various unidimensional and two-dimensional parameters with three-dimensional echocardiographically determined left atrial volume. J Am Soc Echocardiogr 2006;19:1026–32.
31. Jenkins C, Bricknell K, Marwick TH. Use of real-time three-dimensional echocardiography to measure left atrial volume: comparison with other echocardiographic techniques. J Am Soc Echocardiogr 2005;18:991–7.
32. Anderson JL, Horne BD, Pennell DJ. Atrial dimensions in health and left ventricular disease using cardiovascular magnetic resonance. J Cardiovasc Magn Reson 2005;7:671–5.
33. Sievers B, Kirchberg S, Addo M, Bakan A, Brandts B, Trappe HJ. Assessment of left atrial volumes in sinus rhythm and atrial fibrillation using the biplane area-length method and cardiovascular magnetic resonance imaging with TrueFISP. J Cardiovasc Magn Reson 2004;6:855–63.
34. Hudsmith LE, Cheng AS, Tyler DJ, et al. Assessment of left atrial volumes at 1.5 Tesla and 3 Tesla using FLASH and SSFP cine imaging. J Cardiovasc Magn Reson 2007;9:673–9.
35. Hudsmith LE, Petersen SE, Francis JM, Robson MD, Neubauer S. Normal human left and right ventricular and left atrial dimensions using steady state free precession magnetic resonance imaging. J Cardiovasc Magn Reson 2005;7:775–82.
36. Haider AW, Larson MG, Benjamin EJ, Levy D. Increased left ventricular mass and hypertrophy are associated with increased risk for sudden death. J Am Coll Cardiol 1998;32:1454–9.
37. Mor-Avi V, Sugeng L, Weinert L, et al. Fast measurement of left ventricular mass with real-time three-dimensional echocardiography: comparison with magnetic resonance imaging. Circulation 2004;110:1814–8.
38. Myerson SG, Montgomery HE, World MJ, Pennell DJ. Left ventricular mass: reliability of M-mode and 2-dimensional echocardiographic formulas. Hypertension 2002;40:673–8.
39. Grothues F, Smith GC, Moon JC, et al. Comparison of interstudy reproducibility of cardiovascular magnetic resonance with two-dimensional echocardiography in normal subjects and in patients with heart failure or left ventricular hypertrophy. Am J Cardiol 2002;90:29–34.
40. Katz J, Milliken MC, Stray-Gundersen J, et al. Estimation of human myocardial mass with MR imaging. Radiology 1988;169:495–8.
41. Lorenz CH, Walker ES, Morgan VL, Klein SS, Graham TP Jr. Normal human right and left ventricular mass, systolic function, and gender differences by cine magnetic resonance imaging. J Cardiovasc Magn Reson 1999;1:7–21.
42. Bess RL, Khan S, Rosman HS, Cohen GI, Allebban Z, Gardin JM. Technical aspects of diastology: why mitral inflow and tissue Doppler imaging are the preferred parameters? Echocardiography 2006;23:332–9.
43. Ha JW, Oh JK, Redfield MM, Ujino K, Seward JB, Tajik AJ. Triphasic mitral inflow velocity with middiastolic filling: clinical implications and associated echocardiographic findings. J Am Soc Echocardiogr 2004;17:428–31.
44. Garcia MJ, Ares MA, Asher C, Rodriguez L, Vandervoort P, Thomas JD. An index of early left ventricular filling that combined with pulsed Doppler peak E velocity may estimate capillary wedge pressure. J Am Coll Cardiol 1997;29:448–54.
45. Ommen SR, Nishimura RA, Appleton CP, et al. Clinical utility of Doppler echocardiography and tissue Doppler imaging in the estimation of left ventricular filling pressures: a comparative simultaneous Doppler-catheterization study. Circulation 2000;102:1788–94.
46. D'Souza KA, Mooney DJ, Russell AE, MacIsaac AI, Aylward PE, Prior DL. Abnormal septal motion affects early diastolic velocities at the septal and lateral mitral annulus, and impacts on estimation of the pulmonary capillary wedge pressure. J Am Soc Echocardiogr 2005;18:445–53.
47. Hillis GS, Moller JE, Pellikka PA, et al. Noninvasive estimation of left ventricular filling pressure by E/e' is a powerful predictor of survival after acute myocardial infarction. J Am Coll Cardiol 2004; 43:360–7.
48. Maceira AM, Prasad SK, Khan M, Pennell DJ. Normalized left ventricular systolic and diastolic function by steady state free precession cardiovascular magnetic resonance. J Cardiovasc Magn Reson 2006;8:417–26.
49. Kudelka AM, Turner DA, Liebson PR, Macioch JE, Wang JZ, Barron JT. Comparison of cine magnetic resonance imaging and Doppler echocardiography for evaluation of left ventricular diastolic function. Am J Cardiol 1997;80:384–6.
50. Rubinshtein R, Glockner JF, Feng D, et al. Comparison of magnetic resonance imaging versus Doppler echocardiography for the evaluation of left ventricular diastolic function in patients with cardiac amyloidosis. Am J Cardiol 2009;103:718–23.
51. Rathi VK, Doyle M, Yamrozik J, et al. Routine evaluation of left ventricular diastolic function by cardiovascular magnetic resonance: a practical approach. J Cardiovasc Magn Reson 2008;10:36.
52. Nagel E, Stuber M, Burkhard B, et al. Cardiac rotation and relaxation in patients with aortic valve stenosis. Eur Heart J 2000;21:582–9.
53. Edvardsen T, Rosen BD, Pan L, et al. Regional diastolic dysfunction in individuals with left ventricular hypertrophy measured by tagged magnetic resonance imaging—the Multi-Ethnic Study of Atherosclerosis (MESA). Am Heart J 2006;151:109–14.
54. Valeti VU, Chun W, Potter DD, et al. Myocardial tagging and strain analysis at 3 Tesla: comparison with 1.5 Tesla imaging. J Magn Reson Imaging 2006;23:477–80.
55. Petersen SE, Jung BA, Wiesmann F, et al. Myocardial tissue phase mapping with cine phase-contrast MR imaging: regional wall motion analysis in healthy volunteers. Radiology 2006; 238:816–26.
56. Jung B, Foll D, Bottler P, Petersen S, Hennig J, Markl M. Detailed analysis of myocardial motion in volunteers and patients using high-temporal-resolution MR tissue phase mapping. J Magn Reson Imaging 2006;24:1033–9.
57. Bergvall E, Cain P, Arheden H, Sparr G. A fast and highly automated approach to myocardial motion analysis using phase contrast magnetic resonance imaging. J Magn Reson Imaging 2006;23:652–61.
58. Chirillo F, Brunazzi MC, Barbiero M, et al. Estimating mean pulmonary wedge pressure in patients with chronic atrial fibrillation from transthoracic Doppler indexes of mitral and pulmonary venous flow velocity. J Am Coll Cardiol 1997;30:19–26.

JACC: CARDIOVASCULAR IMAGING, VOL. 3, NO. 4, 2010
APRIL 2010:409–20

59. Arques S, Roux E, Sbragia P, et al. Usefulness of bedside tissue Doppler echocardiography and B-type natriuretic peptide (BNP) in differentiating congestive heart failure from noncardiac cause of acute dyspnea in elderly patients with a normal left ventricular ejection fraction and permanent, nonvalvular atrial fibrillation: insights from a prospective, monocenter study. Echocardiography 2007;24:499–507.
60. Okura H, Takada Y, Kubo T, et al. Tissue Doppler-derived index of left ventricular filling pressure, E/E', predicts survival of patients with nonvalvular atrial fibrillation. Heart 2006; 92:1248–52.
61. Uribe S, Tangchaoren T, Parish V, et al. Volumetric cardiac quantification by using 3D dual-phase whole-heart MR imaging. Radiology 2008;248:606-14.
62. Bolger AF, Heiberg E, Karlsson M, et al. Transit of blood flow through the human left ventricle mapped by cardiovascular magnetic resonance. J Cardiovasc Magn Reson 2007;9: 741–7.
63. Iles L, Pfluger H, Phrommintikul A, et al. Evaluation of diffuse myocardial fibrosis in heart failure with cardiac magnetic resonance contrast-enhanced T1 mapping. J Am Coll Cardiol 2008;52:1574–80.

Key Words: echocardiography ■ cardiac magnetic resonance ■ heart failure with normal ejection fraction ■ diastolic heart failure ■ imaging.